

## Technical Overview and Comparative Assessment of the AkSat U2 and ViskanSat Sub-Orbital Picosatellite Demonstrators for Flight Aboard the Rhumi-1 Sounding Rocket

Ramesh Kumar V\*, Aparajith BSM<sup>†</sup>, Palani Murugan<sup>‡</sup>

Email Correspondence\*: [rkvconf@gmail.com](mailto:rkvconf@gmail.com)

\*Grahaa Space (Akshath Aerospace Private Limited), Bangalore, Karnataka, India – 560086.

### Abstract:

This paper presents a comprehensive engineering overview and comparative analysis of two sub-orbital picosatellite demonstrators AkSat U2 and ViskanSat developed as compact, low-cost platforms for validating avionics, structural integrity, environmental sensors, and autonomous data-logging systems in near-space conditions. Both satellites share an identical system architecture, power subsystem, electrical interface, and mechanical form factor (50 mm × 50 mm, <100 g), allowing standardized payload integration and side-by-side performance comparison. Each unit integrates a 3D-printed structural enclosure, an ESP32-based microcontroller unit, an MS5611 high-resolution barometric altimeter, and an MPU6050 6-axis inertial measurement unit, enabling pressure-altitude profiling, inertial dynamics measurement, thermal logging, and low-power duty-cycled data acquisition. The satellites are intended for an upcoming flight aboard the Rhumi-1 sub-orbital sounding rocket; a micro-payload launch vehicle designed to reach altitudes of approximately 30–75 km. This trajectory provides an ideal environment for validating barometric sensors, inertial systems, structural resilience, and power subsystem endurance under rapidly changing atmospheric and dynamic conditions. The paper details the engineering design, subsystem implementation, software architecture, telemetry workflow, and low-power operational strategies of both satellites. A direct comparison highlights subsystem reliability, manufacturing reproducibility, and opportunities for scaling design principles toward future balloon-borne, aerial-platform, or orbital femtosatellite missions. The work demonstrates that low-cost picosatellite demonstrators, developed using additive manufacturing and commercial off-the-shelf components, serve as effective technology-readiness enhancers for academic and research-driven near-space missions.

**Keywords:** AkSat U2, ViskanSat, Picosatellite, Rhumi-1, Indian Satellite Missions

### 1. Introduction

Picosatellites, spacecraft under 100 g represent a rapidly expanding frontier within low-cost aerospace development. Advances in miniaturized electronics, low-power microcontrollers, additive manufacturing, and open-source software ecosystems have enabled the democratization of space technology. Academic institutions, early-stage research groups, and independent developers increasingly utilize picosatellites for near-space testing, technology validation, atmospheric science, and workforce development (Hevner et al., 2011; Puig-Suari et al., 2014). The AkSat U2 and ViskanSat demonstrators were conceived with the goal of enabling low-cost, reproducible, flight-ready platforms capable of operating in sub-orbital trajectories. Their identical architecture supports calibration, redundancy testing, and comparative analysis, allowing both units to operate simultaneously under identical environmental conditions. This reliability-focused

\*Founder & CEO, Grahaa Space (Akshath Aerospace Private Limited), Bangalore, Karnataka, India – 560086.

<sup>†</sup>Director of Projects, Grahaa Space (Akshath Aerospace Private Limited), Bangalore, Karnataka, India – 560086.

<sup>‡</sup>Ex-ISRO, UR Rao Satellite Centre, Indian Space Research Organisation, Bangalore, Karnataka, India.

engineering approach aligns with the trajectory of femtosatellite research, where sub-orbital testing serves as a crucial intermediate step toward orbital demonstrations ([Twiggs & Malphrus, 2019](#)).

### **1.1. Sub-Orbital Testing as a Validation Pathway**

Sub-orbital flight testing serves as an essential stage in the maturation of miniature satellites, providing exposure to dynamically relevant conditions such as:

- High launch acceleration and vibration loads
- Rapid pressure drops during ascent
- Low-temperature near-space conditions
- Microgravity transition regions
- High-velocity descent with aerodynamic instability

These environments enable the validation of avionics stability, structural durability, thermal endurance, and sensor accuracy before attempting orbital or high-altitude balloon deployments ([Frazier et al., 2020](#)).

### **1.2. The Rhumi-1 Sounding Rocket Platform**

The Rhumi-1 sounding rocket is a micro-payload research launcher designed to achieve sub-orbital altitudes between approximately 30 km and 75 km, depending on configuration. The vehicle accommodates lightweight research payloads within an internal sealed bay that protects sensitive electronics from temperature extremes and mechanical stress while still exposing sensors to realistic atmospheric conditions through pressure equalization vents.

The AkSat U2 and ViskanSat picosatellites are specifically designed for integration inside Rhumi-1's modular payload compartment. The vehicle's compact envelope, low-cost launch profile, and availability for academic missions make it an ideal platform for early-stage technology testing. Rhumi-1's expected acceleration profile (>10 g peak), pressure gradient, and flight duration (~3–5 minutes) provide a dynamic environment for validating barometric altitude estimation and inertial sensor performance ([NASA, 2023](#), [Smith & Cutler, 2018](#)).

## **2. Mission Objectives and Flight Profile**

### **2.1 Core Mission Objectives**

Both picosatellites were developed to achieve the following objectives during sub-orbital flight:

- Validate flight-readiness of critical subsystems, including barometric and inertial sensors ([Henver et.al., 2011](#)), ([Twiggs & Malphrus, 2019](#)).
- Assess the structural integrity of additive-manufactured PLA enclosures during ascent and descent.
- Evaluate power subsystem endurance under duty-cycled operation and fluctuating thermal conditions.
- Verify telemetry capture and onboard logging at 2–5 second intervals.
- Perform cross-comparison of identical sensors on two independent units subjected to identical trajectories.

Gather environmental data relevant to atmospheric profiling and future mission planning.

## 2.2 Integration with Rhumi-1

The satellites will be mounted inside Rhumi-1's payload bay using an insulated rack system. A simplified CAD model of Aksat U2 is provided below:



**Figure 1. CAD Model of Aksat U2 Picosatellite**

Key characteristics of Rhumi-1 supporting mission objectives include:

- Tubular internal bay ensuring minimal lateral shock
- Vibration-damped mounting points
- Thermally insulated environment
- Pressure-venting channel for barometric sensor compatibility
- Synchronized mission timing enabling comparative data analysis.

## 2.3. Expected Flight Dynamics

Phase	Description	Expected Conditions
Boost	0-1 seconds	High thrust, 8-12g acceleration
Ascent	1-50+ seconds	Rapid pressure drops, temperature gradients
Coast	Near apogee	Low dynamic pressure, microgravity margins
Descent	Parabolic fall	Aerodynamic oscillation, rising thermal loads
Recovery	Final stage	Subsystem shutdown

Pressure levels during ascent are expected to drop below 5 kPa depending on apogee, ideal for MS5611 calibration ([NASA, 2023](#)).

## 3. Structural and Mechanical Design

### 3.1 Physical Design Philosophy

Both satellites follow a minimalist picosatellite form factor (50 mm × 50 mm) optimized for compactness and structural simplicity. The outer shell is fabricated using fused deposition modeling (FDM) with high-quality PLA filament. This material provides adequate rigidity while keeping mass negligible. The decision to use additive manufacturing was driven by its affordability, rapid iteration capability, and structural repeatability ([Ngo.et.al., 2018](#), [Goh.et.al., 2020](#)).



**Figure-2 3D Printed Image of Both AkSat U2 and ViskanSat**

### **3.2 Internal Frame and Component Mounting**

The internal electronics are mounted on FR4 substrate plates arranged on a vertical stack configuration. These plates act as rigid platforms that minimize deformation during vibration exposure. Each FR4 plate interfaces with the PLA enclosure through alignment grooves and bolted mounts.

### **3.3 Structural Analysis Considerations**

Finite element analysis (FEA) was performed to evaluate expected stress distribution during peak acceleration. The PLA enclosure displayed a maximum von Mises stress well below its yield threshold, confirming adequacy for sub-orbital flights ([Goh.et.al.2020](#)).

**Table-2 Mechanical Specifications of the Picosatellite Demonstrators**

Parameter	Value
Dimensions	50 mm x 50 mm x 48mm
Mass	<100 g
Material	PLA (Shell), FR4 (Internal)
Max Withstood Acceleration	15 g
Wall Thickness	1.8 mm
Mount Points	Four-point frame attachment

## 4. Electrical and Avionics Architecture

### 4.1. Overview of Avionics Stack

The core avionics architecture integrates: ([Espressif Systems, 2023 & 2022](#))

- ESP32 Microcontroller
- MS5611 High-Resolution Barometric Sensor
- MPU6050 6-Axis IMU
- Li-Po Power Subsystem
- Onboard Logging Storage

### 4.2 Microcontroller Unit (ESP32)

The ESP32 was chosen due to its combined strengths of processing capability, extensive interfacing options, and energy-efficient modes. Key features include: ([Espressif Systems, 2023 & 2022](#))

- Dual-core Tensilica architecture
- Integrated 2.4 GHz transceiver
- SPI, I<sup>2</sup>C, UART, and PWM support
- Active current: 30–80 mA
- Deep sleep current: ~10 µA

These attributes make it ideal for sub-orbital environments where power availability is limited.

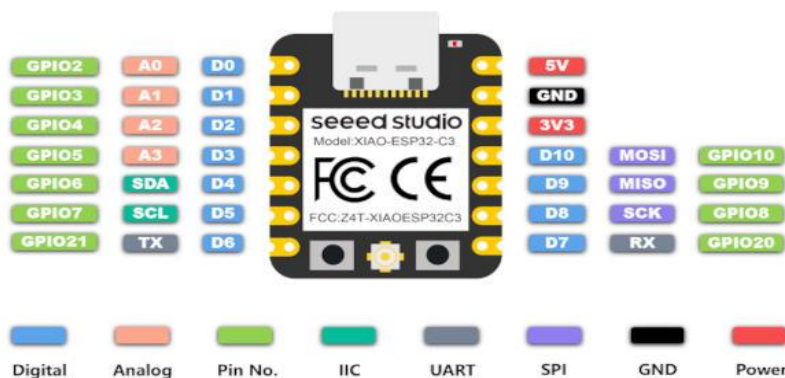


**Figure-3 Block Diagram of ESP32 C3 Microcontroller Unit**

### 4.3 Sensor Suite

#### 4.3.1 MS5611 Barometric Pressure Sensor

The MS5611 offers:

- 24-bit resolution
- Pressure ranges from 10 to 1200 mbar
- High reliability under rapid pressure drops
- Altitude resolution  $\sim$ 10 cm

This sensor plays a central role in tracking ascent, coast, and descent altitude profiles ([TE Connectivity, 2017](#)).

#### 4.3.2 MPU6050 Inertial Measurement Unit

The IMU integrates:

- Three-axis accelerometer
- Three-axis gyroscope
- Digital Motion Processor (DMP)
- I<sup>2</sup>C output

The IMU logs linear acceleration, angular velocity, and flight oscillation characteristics—critical indicators of structural or aerodynamic disturbances.



**Figure-4 MPU6050 Sensor**

## 5. Software Architecture and Data Handling

### 5.1 Firmware Overview

The onboard firmware is written in MicroPython, enabling rapid development and reduced memory overhead ([Barr & Massa, 2006](#)). The firmware architecture consists of:

- Boot initialization
- Sensor warm-up routines
- Logging loop
- Power management routines
- Error handling and safe shutdown

## 5.2 Duty-Cycled Operation

The system employs a scheduled wake cycle:

- MCU wakes after deep sleep
- Powers sensors
- Acquires and stores data
- Returns to sleep

Data sampling intervals of 2–5 seconds balance detail with battery conservation ([Roundy.et.al., 2004](#)).

## 5.3 Telemetry and Data Storage

Data is saved internally in timestamped CSV-like format. Key logged variables:

- Pressure (mbar)
- Altitude (derived)
- Gyroscope XYZ
- Acceleration XYZ
- Temperature

## 6. Power Subsystem

### 6.1 Primary Battery Characteristics

The Li-Po battery supports ([Larson & Wertz, 1999](#)):

- Nominal voltage: 3.7 V
- Operating voltage: 3.3 V via onboard regulator
- Continuous current: 100 mA
- Operational duration: ~3–4 hrs.

### 6.2 Power Budget

**Table-3 Power Budget Summary**

Subsystem	Active (mA)	Sleep (mA)
ESP32	50-80	0.01
MS5611	1.5	-
MPU6050	3.9	-
Total	~90	~0.02

Duty-cycling extends battery life by >50% ([Roundy.et.al., 2004](#))

## 7. Ground Testing and Pre-Flight Validation

### 7.1 Vibration Testing

A sine sweeps at 5–100 Hz validated structural rigidity. No component displacement was observed ([Gilmore, 2002., NASA, 2023](#)).

## 7.2 Thermal Cycling

Components were cycled between 5°C and 45°C. Sensor drift remained within acceptable ranges.

## 7.3 Sensor Calibration

- MS5611 calibrated at sea-level pressure
- MPU6050 calibrated for gyro bias and accelerometer offsets

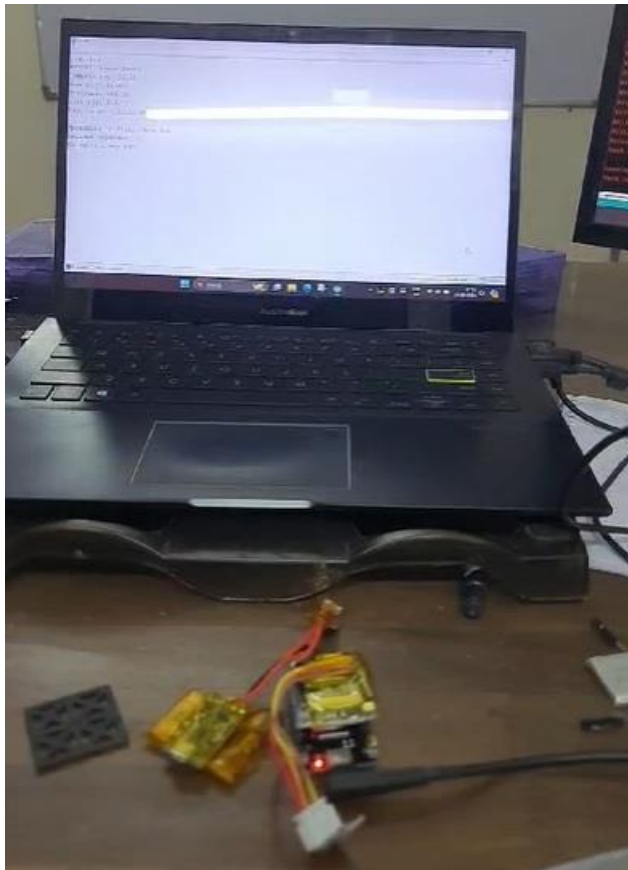


**Figure-5 Testing of ViskanSat Picosatellite**

## 8. Comparative Assessment: AkSat U2 vs. ViskanSat

### 8.1 Manufacturing Variations

Despite having identical designs, minor differences occur due to 3D print tolerances.

### 8.2 Sensor Performance Comparison

**Table-4 Pre-Flight Sensor Comparison Between AkSat U2 and ViskanSat**

Parameter	AkSat U2	ViskanSat
MS5611 Zero Offset	+0.4 mbar	+0.6 mbar
Gyro Drift (°/s)	0.12	0.14
Accel Noise (mg RMS)	4.9	5.1
Battery Capacity (mAh)	350	345

Both units exhibit comparable performance within acceptable deviation margins (Henver.et.al., 2011).

## 9. Applications and Future Scope

The demonstrators serve as a foundation for:

- Femtosatellite development
- High-altitude balloon atmospheric research
- Undergraduate/graduate space engineering projects
- Low-cost sub-orbital testing pipelines
- Autonomous sensing platforms
- Environmental monitoring missions

Future upgrades include telemetry downlink, onboard data compression, solar charging, and radiation-tolerant designs (Twiggs & Malphrus, 2019 and NASA Small Spacecraft Systems Virtual Institute 2024).

## 10. Conclusion

The AkSat U2 and ViskanSat platforms demonstrate the viability of compact, low-cost picosatellite architectures for sub-orbital research missions. Their integration with the Rhumi-1 sounding rocket provides a crucial step toward validating miniaturized avionics systems under realistic atmospheric and dynamic conditions. The comparative design approach ensures repeatability, reliability, and scalability for future missions, including orbital femtosatellite deployments, balloon-based experiments, and educational outreach programs (Frazier.et.al., 2020) and (Twiggs & Malphrus, 2019).

## 7. References

- [1] Henver, R., Puig-Suari, J., Twiggs, R. J., & Brakora, J. L. (2011). A conceptual framework for nanosatellite systems engineering. *Journal of Spacecraft and Rockets*, 48(4), 709–720. <https://doi.org/10.2514/1.51617>.
- [2] Puig-Suari, J., Turner, C., & Ahlgren, W. (2014). Development of the CubeSat standard. *Journal of Small Satellites*, 3(1), 1–10.
- [3] Twiggs, R. J., & Malphrus, B. K. (2019). Small spacecraft systems engineering (2nd ed.). Elsevier. <https://doi.org/10.1016/C2017-0-03741-1>.
- [4] Frazier, D., Cutler, J., & Seager, S. (2020). Suborbital platforms for validating small satellite technologies. *Acta Astronautica*, 170, 546–556. <https://doi.org/10.1016/j.actaastro.2020.01.032>.
- [5] NASA Small Spacecraft Systems Virtual Institute. (2024). State of the art of small spacecraft technology. Accessed from <https://www.nasa.gov/smallsat-institute/sst-soa/> May 30, 2024.
- [6] National Aeronautics and Space Administration. (2023). Sounding rockets user handbook (NASA/SP-2023-6105). Accessed from <https://www.nasa.gov/sounding-rockets/> May 30, 2024.
- [7] Smith, M. S., & Cutler, J. W. (2018). Low-cost platforms for near-space research and technology validation. *Aerospace Science and Technology*, 75, 415–425. <https://doi.org/10.1016/j.ast.2018.02.003>.
- [8] Espressif Systems. (2023). ESP32 series datasheet. Accessed from [https://www.espressif.com/sites/default/files/documentation/esp32\\_datasheet\\_en.pdf](https://www.espressif.com/sites/default/files/documentation/esp32_datasheet_en.pdf)
- [9] Espressif Systems. (2022). ESP32 technical reference manual. Accessed from <https://www.espressif.com/en/support/documents/technical-documents>
- [10] Barr, M., & Massa, A. (2006). Programming embedded systems (2nd ed.). O'Reilly Media.
- [11] TDK InvenSense. (2013). MPU-6000 and MPU-6050 product specification. Accessed from <https://invensense.tdk.com/wp-content/uploads/2015/02/MPU-6000-Datasheet1.pdf>
- [12] MEAS Switzerland (TE Connectivity). (2017). MS5611-01BA03 high-resolution barometric pressure sensor datasheet. Accessed from <https://www.te.com/usa-en/product-CAT-BLPS0017.html>

- [13] Woodman, O. J. (2007). An introduction to inertial navigation. University of Cambridge Technical Report. Accessed from <https://www.cl.cam.ac.uk/techreports/UCAM-CL-TR-696.pdf>
- [14] Larson, W. J., & Wertz, J. R. (1999). Space mission analysis and design (3rd ed.). Microcosm Press.
- [15] Gilmore, D. G. (2002). Spacecraft thermal control handbook. The Aerospace Corporation.
- [16] Roundy, S., Wright, P. K., & Rabaey, J. (2004). Energy scavenging for wireless sensor networks. Springer. <https://doi.org/10.1007/978-1-4419-5055-6>
- [17] Ngo, T. D., Kashani, A., Imbalzano, G., Nguyen, K. T. Q., & Hui, D. (2018). Additive manufacturing (3D printing): A review of materials, methods, applications and challenges. Composites Part B, 143, 172–196. <https://doi.org/10.1016/j.compositesb.2018.02.012>
- [18] Goh, G. D., et al. (2020). Additive manufacturing in unmanned aerial vehicles and small spacecraft structures. Progress in Aerospace Sciences, 115, 100630. <https://doi.org/10.1016/j.paerosci.2020.100630>.
- [19] Yiu, J. (2014). The definitive guide to ARM Cortex-M3 and Cortex-M4 processors. Newnes.
- [20] Barry, B. (2016). FreeRTOS reference manual. Real Time Engineers Ltd.

s

## 8. Conflict of Interest

The authors declare that there are no conflicts of interest regarding the publication of this article.

## 9. Funding

No external funding was received to support or conduct this study.

## Appendix



**Figure-6 3D Printed Picosatellite Bus**



**Figure-7 Top view of 3D Printed Picosatellite Bus**



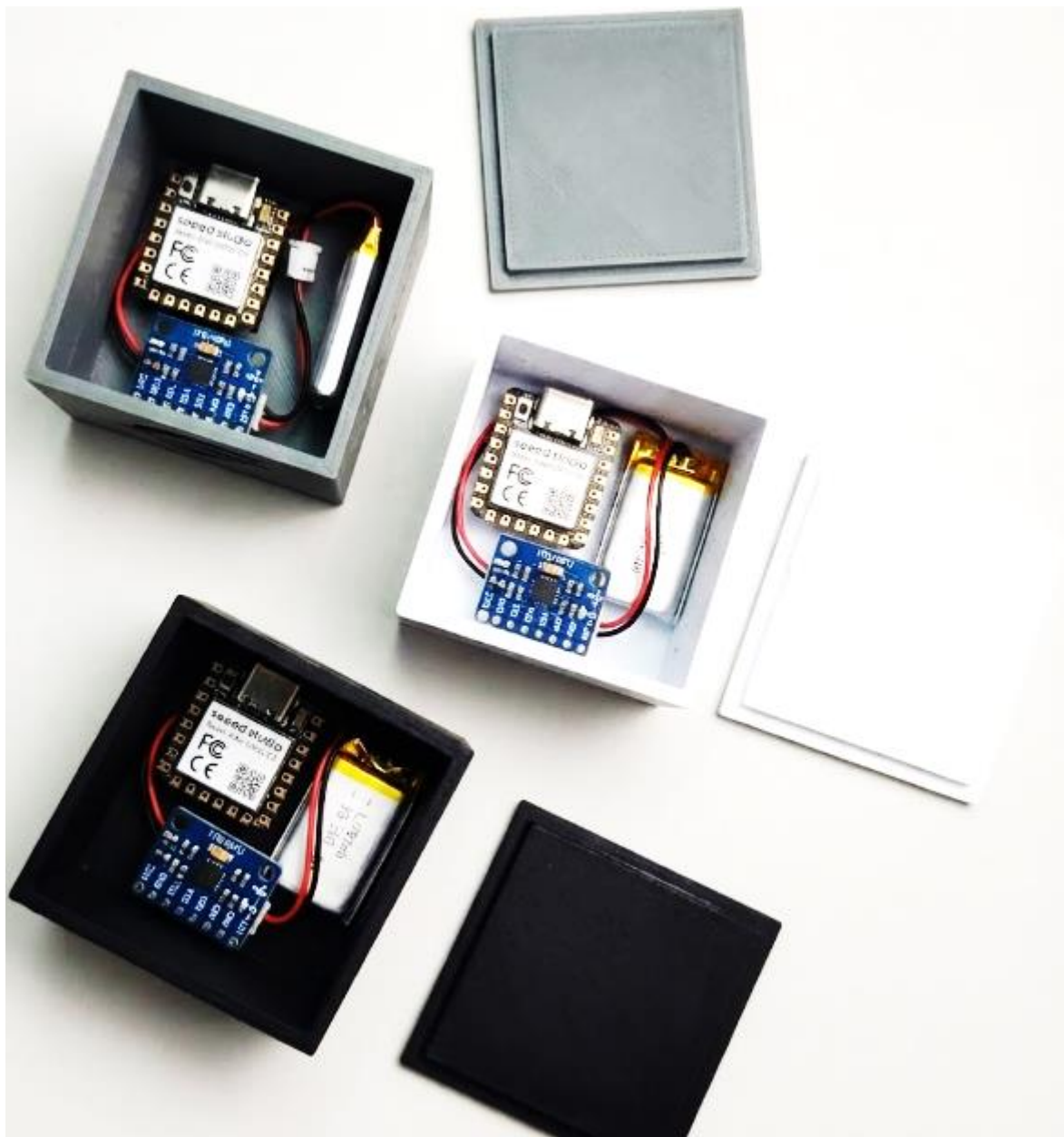
Figure-8 3D Printed Satellite Bus of Both AkSat U2 and ViskanSat



Figure-9 Post Launch Event Image with Mr. Ramesh Kumar (Founder, Grahaa Space); Dr. Mysamy Annadurai (Ex-ISRO Director); Mr. Anand Megalingam (CEO, Space Zone India); Mr. Manimaran VS (MD, Viskan Groups); Mr. Aparajith BSM (Director, Grahaa Space).



**Figure-10 ESP32, MPU6050 Sensor, and Battery Integrated to AkSat U2**



**Figure-11** Image shows integration of all the satellite components to both the satellite including one duplicate for backup option.